

# PERFORMANCE OF TRELIS CODED QPSK IN MOBILE RADIO CHANNELS

Said El-Noubi, Eman Fahmy and El-Sayed El-Badawy

Department of Electrical Engineering, Faculty of Engineering,  
Alexandria University, Alexandria, Egypt.

## ABSTRACT

The performance of Trellis coded QPSK in Mobile radio communication channels characterized by fast Rayleigh fading is studied using Mont Carlo simulation. The receiver consists of one-bit and two-bit differential detectors followed by Viterbi decoding. Previously published work showed that using this receiver improves the bit error rate of QPSK in additive white Gaussian noise channels. However, the performance of this receiver in fast Rayleigh fading has not been studied yet. In this paper we present simulation studies of this receiver to detect 4-state Trellis coded QPSK in fast Rayleigh fading. The mobile radio channel simulator using FIR digital filter is described. Simulation results computed by Mont Carlo counting techniques are presented at different fading rates and signal-to-noise ratios.

## INTRODUCTION

Trellis coded modulation (TCM) [1] has been proposed for high speed voice-band data transmission [2]. Recently, application to mobile radio and mobile satellite systems was also proposed in [3-5]. It was reported in [3] that multiple differential detectors as well as interleaving can improve the bit error rate (BER) performance of differentially detected TCM. The BER results obtained using Mont Carlo simulation were presented there for different configurations of differential detection and interleaving. In [4], a sequential decoder was developed to improve the BER in white Gaussian noise channels. More receiver structures were introduced in [6] to improve the BER of differentially detected MSK and QPSK systems using the one- and two-bit differential detector outputs for maximum likelihood sequence estimation. However, the BER performances of these receivers were studied in additive white Gaussian noise (AWGN) channels only.

In [7], we had studied the performance of two-state trellis coded 4 differential phase shift keying (4-DPSK) system in mobile radio channels.

In this paper, we investigate the performance of four-state trellis coded differential quadrature phase shift keying (DQPSK) with a combination of one-bit and two-bit differential detectors followed by Viterbi decoding. A channel simulator using Finite Impulse Response (FIR) digital filter is introduced. Different fading rates are studied by varying the filter coefficients.

In section II, the signal and system models are described. In section III, the UHF mobile radio channel simulation using digital filtering is described. In section IV, the receiver performance is analyzed and the basic

simulation equations are derived. Finally, simulation results are presented in section V.

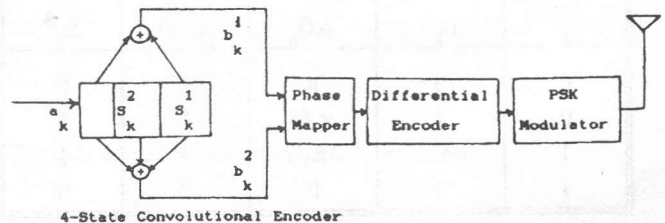


Figure 1. Block diagram of the trellis coded QPSK modulator.

## SIGNAL AND SYSTEM MODEL

The transmitter was described in detail in [4] and is shown in Figure (1). It consists of a convolutional encoder with rate 1/2, and has 2-past bits, a phase mapper, a differential encoder and a PSK modulator. The input to the 4-state convolutional encoder is an equiprobable independent binary sequence  $a_k = 0$  or 1.

For each input bit  $a_k$ , the convolution encoder produces two output bits  $b_k^1$  and  $b_k^2$  where:

$$b_k^1 = a_k \oplus a_{k-2} \quad (1)$$

and

$$b_k^2 = a_k \oplus a_{k-1} \oplus a_{k-2}$$

Figure (2) shows the trellis diagram for the convolutional coding. The phase mapper converts the code binary sequence into M-ary PSK symbols as follows [4]:

$$c_k = e^{j\Delta\theta_k} \quad (2)$$

where

$$\Delta\theta_k = \{b_k^2 + [(4-(3)b_k^2) b_k^1] + [3-(5)b_k^1]\}(\pi/2) \quad (3)$$

The output of the PSK modulator is given by

$$s_\sigma(t) = \cos(\omega_c t + \theta_k); \quad kT < t < (k+1)T \quad (4)$$

where

$$\theta_k = \Delta\theta_k \oplus \theta_{k-1} \quad \text{mod } 2\pi.$$

The phase difference can be expressed as

$$\theta(kT) - \theta(kT-T) = m(k) (\pi/2) \quad (5)$$

where

$$m(k) = 0, 1, 2, \text{ or } 3.$$

Table I shows the relationships between  $b_k^2$ ,  $b_k^1$ ,  $m(k)$  and  $S_k^2$ .

Table 1.

$b_k^2$	$b_k^1$	$\Delta\theta_k$	$m(k)$	$S_k^2$
0	0	$\pi$	2	0
0	1	$\pi/2$	1	1
1	0	$3\pi/2$	3	1
1	1	0	0	0

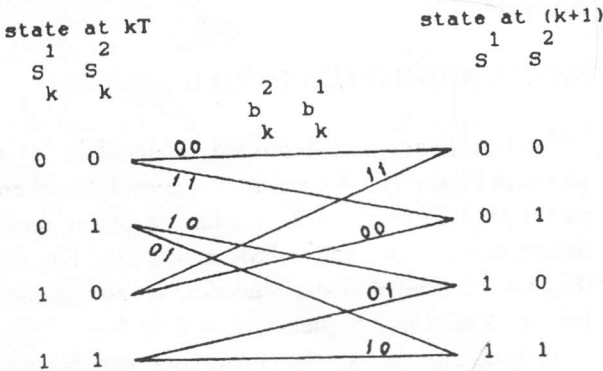


Figure 2. Trellis diagram of the convolutional coding.

MOBILE RADIO CHANNEL SIMULATION

The UHF mobile radio channel is characterized by multiple signal paths between the transmitter and receiver due to reflections from buildings, terrain, and other scattering structures. This causes signal fading. The rate at

which the signal envelope fades is directly proportional to the speed of the mobile receiver [8].

Analytically, this observation manifests itself as Doppler frequency shift associated with each signal component. Due to the Doppler effect, a transmitted single frequency carrier results in multiple signals at the receiver having comparable amplitudes, random phases, and relative frequency shifts confined to the Doppler spread about the carrier frequency. The power spectrum of the Rayleigh fading signal is shown in Figure (3) and can be expressed as

$$S_F(f) = \frac{E^2}{2\pi\sqrt{f_D^2 - f^2}} \quad |f| < f_D \quad (6)$$

$$= 0 \quad \text{otherwise}$$

where E is the rms value of the signal envelope,  $f_D$  is the maximum Doppler shift.

The spectrum depicted in Figure (3) is simulated by passing white Gaussian noise through a shaping filter whose squared magnitude response approximates the spectrum of the Doppler shift [9]. We selected a Finite Impulse Response (FIR) digital filter designed by the frequency sampling techniques [10] summarized in the following. Assuming that the FIR digital filter has impulse response duration of k samples, then the filter transfer function  $H_F(z)$  is given by

$$H_F(z) = \sum_{k=0}^{K-1} h_F(k) z^{-k} \quad (7)$$

where  $h_F(k)$ ,  $k = 0, 1, 2, \dots, K-1$  are the filter coefficients.

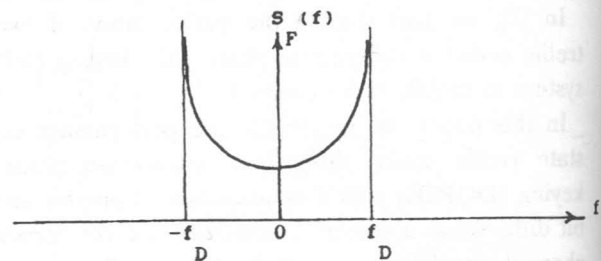


Figure 3. Power spectrum of the received in-phase and quadrature-phase signals.

They are calculated from the samples  $H_F(n)$ ,  $n = 0, 1, 2, \dots, K-1$  of the frequency response as follows

$$h_F(k) = \frac{1}{K} \sum_{n=0}^{K-1} \tilde{H}_F(n) e^{j2\pi kn/K} \quad (8)$$

where  $\tilde{H}_F(n) = H_F(e^{j2\pi n/K})$

K was taken equal to 1000 samples equally spaced in frequency between 0 and  $2\pi$  in our simulations.

We considered the cases  $f_D T = 0, .001, .003$  and  $.005$  and calculated the filter coefficients in each case, then evaluated the frequency response and compared it with the desired response to make sure that the approximation is good.

Two independent Gaussian sequences  $v(kT)$  and  $u(kT)$  are generated by passing two independent white Gaussian noise sequences  $G1(kT)$  and  $G2(kT)$  through this filter.

Therefore,

$$v(kT) = \sum_{c=0}^k G1(cT) h_F((k-c)T) \quad (9)$$

$$u(kT) = \sum_{c=0}^k G2(cT) h_F((k-c)T)$$

The sequences  $v(kT)$  and  $u(kT)$  are used to simulate the received faded signal at the receiver.

RECEIVER PERFORMANCE ANALYSIS AND SIMULATION

The signal  $x_r(t)$  at the input of the receiver can be represented as

$$x_r(t) = v(t) \cos(\omega_c t + \theta_k) - u(t) \sin(\omega_c t + \theta_k) + n_{white}(t) \quad (10)$$

$kT < t < (k+1)T$

where  $v(t)$  and  $u(t)$  are independent lowpass Gaussian processes with the spectrum shown in Figure (3) and  $n_{white}(t)$  is white Gaussian noise. The receiver block diagram is shown in Figure (4) and has been described in detail in [6]. Assuming that the IF filter has a Gaussian transfer function and a bandwidth much bigger than the maximum Doppler shift, the output  $y(t)$  can be expressed as

$$y(t) = v(t) \cos(\omega_c t + \theta_k) - u(t) \sin(\omega_c t + \theta_k) + n_o(t) \quad (11)$$

and

$$n_o(t) = n_c(t) \cos(\omega_c t) - n_s(t) \sin(\omega_c t) \quad (12)$$

where  $n_c(t)$  and  $n_s(t)$  are i.i.d. lowpass Gaussian processes having Gaussian spectra. They can be generated by passing two i.i.d. white Gaussian noises  $G3(t)$  and  $G4(t)$  through a lowpass filter of Gaussian impulse response  $h_{Gauss}(t)$ .

$$n_c(t) = G3(t) * h_{Gauss}(t) \quad (13)$$

$$n_s(t) = G4(t) * h_{Gauss}(t)$$

where \* denotes convolution.

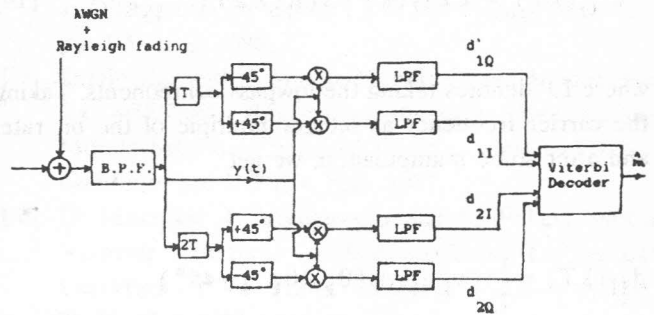


Figure 4. Block diagram of the receiver.

In the simulation, two corresponding sequences  $n_c(kT)$  and  $n_s(kT)$  are generated by discrete convolution

$$n_{c,s}(kT) = \sum_{i=0}^k G_{3,4}(i) h_{Gauss}((k-i)T) \quad (14)$$

Let the subscript k denotes the sample at  $t = kT$ , then

$$y(kT) = v(kT) \cos(\omega_c kT + \theta_k) - u(kT) \sin(\omega_c kT + \theta_k) + n_o(kT) \quad (15)$$

where

$$n_o(kT) = n_c(kT) \cos(\omega_c kT) - n_s(kT) \sin(\omega_c kT) \quad (16)$$

Delaying the signal by a T second and shifting the carrier by  $\pm \pi/4$  yields

$$y(kT-T)_{\pm 45^\circ} = v(kT-T) \{ \cos(\omega_c(kT-T) + \theta(kT-T) \pm 45^\circ) \} - u(kT-T) \{ \sin(\omega_c(kT-T) + \theta(kT-T) \pm 45^\circ) \} + n_o(kT-T)_{\pm 45^\circ} \quad (17)$$

where

$$n_o(kT-T)_{\pm 45^\circ} = n_c(kT-T) \{ \cos(\omega_c(kT-T) \pm 45^\circ) \} - n_s(kT-T) \{ \sin(\omega_c(kT-T) \pm 45^\circ) \} \quad (18)$$

The outputs from the differential detectors are given by

$$\begin{aligned} d_{1I}(kT) &= LP\{y(kT) y(kT-T)\}_{+45^\circ} \\ d_{1Q}(kT) &= LP\{y(kT) y(kT-T)\}_{-45^\circ} \\ d_{2I}(kT) &= LP\{y(kT) y(kT-2T)\}_{+45^\circ} \\ d_{2Q}(kT) &= LP\{y(kT) y(kT-2T)\}_{-45^\circ} \end{aligned} \quad (19)$$

where LP denotes taking the lowpass components. Taking the carrier frequency as integer multiple of the bit rate, and after some manipulation, we get

$$\begin{aligned} d_{1I}(kT) &= \frac{1}{2} v_k v_{k-1} \cos(\theta_k - \theta_{k-1} - 45^\circ) \\ &\quad - \frac{1}{2} v_k u_{k-1} \sin(-(\theta_k - \theta_{k-1} - 45^\circ)) \\ &\quad - \frac{1}{2} u_k v_{k-1} \sin(\theta_k - \theta_{k-1} - 45^\circ) \\ &\quad + \frac{1}{2} u_k u_{k-1} \cos(\theta_k - \theta_{k-1} - 45^\circ) \\ &\quad + \sum_{l=1}^4 \{ n_l(kT) n'_l(kT-T) \}_{+45^\circ} \end{aligned} \quad (20-a)$$

$$\begin{aligned} d_{1Q}(kT) &= \frac{1}{2} v_k v_{k-1} \cos(\theta_k - \theta_{k-1} + 45^\circ) \\ &\quad - \frac{1}{2} v_k u_{k-1} \sin(-(\theta_k - \theta_{k-1} + 45^\circ)) \\ &\quad - \frac{1}{2} u_k v_{k-1} \sin(\theta_k - \theta_{k-1} + 45^\circ) \\ &\quad + \frac{1}{2} u_k u_{k-1} \cos(\theta_k - \theta_{k-1} + 45^\circ) \\ &\quad + \sum_{l=1}^4 \{ n_l(kT) n'_l(kT-T) \}_{-45^\circ} \end{aligned} \quad (20-b)$$

$$\begin{aligned} d_{2I}(kT) &= \frac{1}{2} v_k v_{k-2} \cos(\theta_k - \theta_{k-2} - 45^\circ) \\ &\quad - \frac{1}{2} v_k u_{k-2} \sin(-(\theta_k - \theta_{k-2} - 45^\circ)) \\ &\quad - \frac{1}{2} u_k v_{k-2} \sin(\theta_k - \theta_{k-2} - 45^\circ) \\ &\quad + \frac{1}{2} u_k u_{k-2} \cos(\theta_k - \theta_{k-2} - 45^\circ) \\ &\quad + \sum_{l=1}^4 \{ n_l(kT) n'_l(kT-2T) \}_{+45^\circ} \end{aligned} \quad (20-c)$$

$$\begin{aligned} d_{2Q}(kT) &= \frac{1}{2} v_k v_{k-2} \cos(\theta_k - \theta_{k-2} + 45^\circ) \\ &\quad - \frac{1}{2} v_k u_{k-2} \sin(-(\theta_k - \theta_{k-2} + 45^\circ)) \\ &\quad - \frac{1}{2} u_k v_{k-2} \sin(\theta_k - \theta_{k-2} + 45^\circ) \\ &\quad + \frac{1}{2} u_k u_{k-2} \cos(\theta_k - \theta_{k-2} + 45^\circ) \\ &\quad + \sum_{l=1}^4 \{ n_l(kT) n'_l(kT-2T) \}_{-45^\circ} \end{aligned} \quad (20-d)$$

where

$$\begin{aligned} \sum_{l=1}^4 \{ n_l(kT) n'_l(kT-T) \}_{\pm 45^\circ} &= [\frac{1}{2} v_k \cos(\pm 45^\circ - \theta_k) \\ &\quad + \frac{1}{2} u_k \sin(\pm 45^\circ - \theta_k) + \frac{1}{2} n_{c_k} \cos(\pm 45^\circ) + \frac{1}{2} n_{s_k} \sin(\pm 45^\circ)] n_{c_{k-1}} \\ &\quad + [-\frac{1}{2} v_k \sin(\pm 45^\circ - \theta_k) + \frac{1}{2} u_k \cos(\pm 45^\circ - \theta_k) \\ &\quad - \frac{1}{2} n_{c_k} \sin(\pm 45^\circ) + \frac{1}{2} n_{s_k} \cos(\pm 45^\circ)] n_{s_{k-1}} \\ &\quad + \frac{1}{2} n_{c_k} [v_{k-1} \cos(-\theta_{k-1} - (\pm 45^\circ)) + u_{k-1} \sin(-\theta_{k-1} - (\pm 45^\circ))] \\ &\quad + \frac{1}{2} n_{s_k} [v_{k-1} \sin(-\theta_{k-1} - (\pm 45^\circ)) + u_{k-1} \cos(-\theta_{k-1} - (\pm 45^\circ))] \end{aligned} \quad (21)$$

and

$$\begin{aligned} \sum_{l=1}^4 \{ n_l(kT) n'_l(kT-2T) \}_{\pm 45^\circ} &= [\frac{1}{2} v_k \cos(\pm 45^\circ - \theta_k) \\ &\quad + \frac{1}{2} u_k \sin(\pm 45^\circ - \theta_k) + \frac{1}{2} n_{c_k} \cos(\pm 45^\circ) + \frac{1}{2} n_{s_k} \sin(\pm 45^\circ)] n_{c_{k-2}} \\ &\quad + [-\frac{1}{2} v_k \sin(\pm 45^\circ - \theta_k) + \frac{1}{2} u_k \cos(\pm 45^\circ - \theta_k) \\ &\quad - \frac{1}{2} n_{c_k} \sin(\pm 45^\circ) + \frac{1}{2} n_{s_k} \cos(\pm 45^\circ)] n_{s_{k-2}} \\ &\quad + \frac{1}{2} n_{c_k} [v_{k-2} \cos(-\theta_{k-2} - (\pm 45^\circ)) + u_{k-2} \sin(-\theta_{k-2} - (\pm 45^\circ))] \\ &\quad + \frac{1}{2} n_{s_k} [v_{k-2} \sin(-\theta_{k-2} - (\pm 45^\circ)) + u_{k-2} \cos(-\theta_{k-2} - (\pm 45^\circ))] \end{aligned} \quad (22)$$

Knowing the quantities  $d_{1I}(kT)$ ,  $d_{1Q}(kT)$ ,  $d_{2I}(kT)$  and  $d_{2Q}(kT)$ , the four state Viterbi decoder finds the trellis path of maximum likelihood by estimating  $m(k)$  or  $\Delta\theta_k$  and then  $S_k^1 S_k^2$  (see Table I).

In other words, the decoder uses a maximum likelihood sequence estimation (MLSE) algorithm to find the symbol sequence which is closest to the received signal. This algorithm has been described in detail in [6] and was used in our simulations.

## SIMULATION RESULTS

Each simulation uses a known pseudorandom binary sequence  $\{a_k\}$ .

The other sequences required  $\{u_k\}$ ,  $\{v_k\}$ ,  $\{n_{ck}\}$ , and  $\{n_{sk}\}$  are generated by filtering white Gaussian noise sequences as described in the previous sections.

The sequences  $\{d_{1I}\}$ ,  $\{d_{1Q}\}$ ,  $\{d_{2I}\}$  and  $\{d_{2Q}\}$  are then computed from the equation derived in the previous section. The decoding algorithm estimates the sequence  $\{\hat{m}(k)\}$  and the corresponding data sequence  $\{\hat{a}_k\}$ . The error rate is calculated by counting the number of disagreements between the sequences  $\{\hat{a}_k\}$  and  $\{a_k\}$  and dividing it by the sequence length. The simulation process is repeated many times to find the average bit error rate. The results are shown in Figure (5). It is concluded that the performance of the receiver proposed in [6] is good in mobile radio channels.

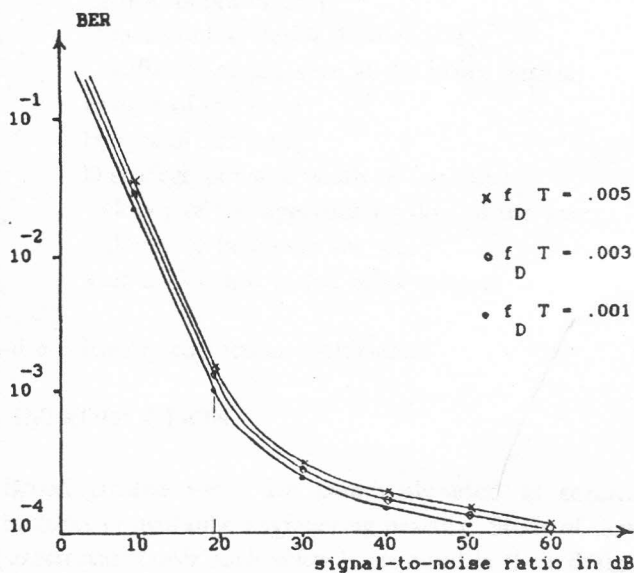


Figure 5. BER results.

## REFERENCES

- [ 1 ] G. Ungerboeck, "Channel Coding With Multilevel Phase Signals", *IEEE Trans. on Information Theory*, pp. 55-67, Jan. 1982.
- [ 2 ] H.K. Thapar, "Real-Time Application of Trellis Coding to High Speed Voiceband Data Transmission", *IEEE J. Selected Areas Communications*, Sept. 1984.
- [ 3 ] D. Makrakis, A. Yongaçoglu and K. Feher, "Interleaving for Differential Detection Using Multiple Detectors", *VTC'88, Philadelphia, PA*, pp. 18-21, June 1988.
- [ 4 ] D. Makrakis and K. Feher, "On Optimal Detection of Noncoherent Trellis coded Modulation Signals, Part 1: Differential Detection", *VTC'88 Philadelphia, PA*, pp. 1-5, June 1988.
- [ 5 ] D. Divsalar and K. Simon, "Trellis Coded Modulation for 4800-9600 Bits/s Transmission Over Fading Mobile Satellite Channels", *IEEE J. Selected Areas Commun*, pp. 162-174, Feb. 1987.
- [ 6 ] D. Makrakis A. Yongaçoglu and K. Feher, "Novel Receiver Structures for Systems Using Differential Detection", *IEEE Trans. on Vehic. Technology*, pp. 71-77, May 1987.
- [ 7 ] Said Elnoubi, Eman Fahmy and El-Sayed El-Badawy, "Two-State Trellis Coded 4-DPSK in Mobile Radio Channels", *Alexandria Engineering Journal Vol. 30, No. 1*, January 1991.
- [ 8 ] W.C. Jakes, "Microwave Mobile Communcaitions", *Wiley, New York*, 1974.
- [ 9 ] E. Caples, K. Massad and T. Minor, "A UHF Channel Simulator for Digital Mobile Radio", *IEEE Trans. on Vehic. Technology*, pp. 281-289, May 1980.
- [ 10 ] A. Oppenheim and R. Schaffer, "Digital Signal Processing", *Prentice Hall*, pp. 251-255, 1975.